Electromagnetic Form Factors of Baryons in the Perturbative Chiral Quark Model

Khanchai Khosonthongkee, Xuyang Liu,
Ayut Limphirat, Yupeng Yan

School of Physics, Institute of Science, Suranaree University of Technology
Nakhon Ratchasima 30000,Thailand

OUTLINE

- Introduction
- Electromagnetic form factor in the Perturbative Chiral Quark Model (PCQM)
- Model quark wave function
- Results & Discussion

1. Introduction

Quantum ChromoDynamics (QCD)

QCD is a fundamental theory of the strong interaction.

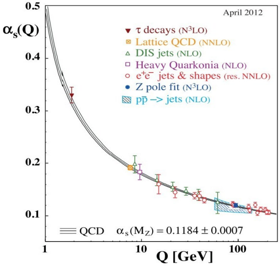

Particle Data Group: 2012

At high energy

QCD is perturbative $\Rightarrow$ asymptotic freedom.

At low energy

QCD is non-perturbative $\Rightarrow$ α_s is large.

Approaches

- Lattice QCD
- Quark Models
- Chiral Perturbation Theory
- $\cdots$

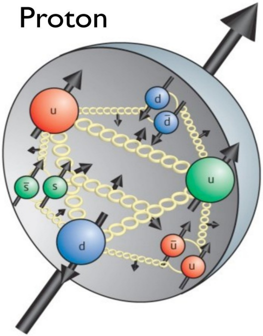

Quark Model

- Baryons are considered as colorless bound states of three constituent quarks.
- The constituent quarks are confined and interacted by effective interactions.

Historically

- MIT Bag Model (PRD**9** 3471(1980); PRD**10** 2599(1980).)
- Chiral Quark Model (PRD**22** 2838(1980); PRD**24** 216(1981))
- ...

Perturbative chiral quark model

PRD**22** 2838(1980); NPA**426** 456(1984); PLB**229** 333(1989);PRC**64** 065203(2001); PRD**63** 054026(2001);

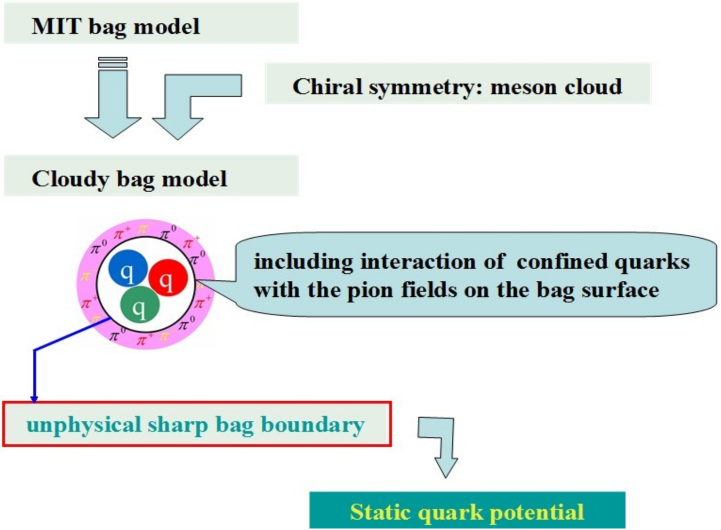

Perturbative Chiral Quark Model (PCQM)

- Three-quark core: quarks as relativistic fermions
- Chiral symmetry: pseudoscalar meson cloud (π, K, η)
- A static quark potential

Previous work in the PCQM

PRC**64** 065203(2001); PRD**63** 054026(2001); PLB**520** 204(2001); PRC**65** 025202(2002); PRC**66** 055204(2002); PRC**68** 015205(2003); EPJA**20** 317(2004); JPG**30** 793(2004); JPG**35** 025005(2008).

- electromagnetic properties of baryons
- low-energy meson-baryon scattering
- strange nucleon form factors
- electromagnetic excitation of nucleon resonances
- axial form factor of the nucleon
- ......

Axial and EM FFs in the PCQM

J. Phys. G: Nucl. Part. Phys. **30** 793 (2004). Eur. Phys. J. A **20**, 317 (2004).

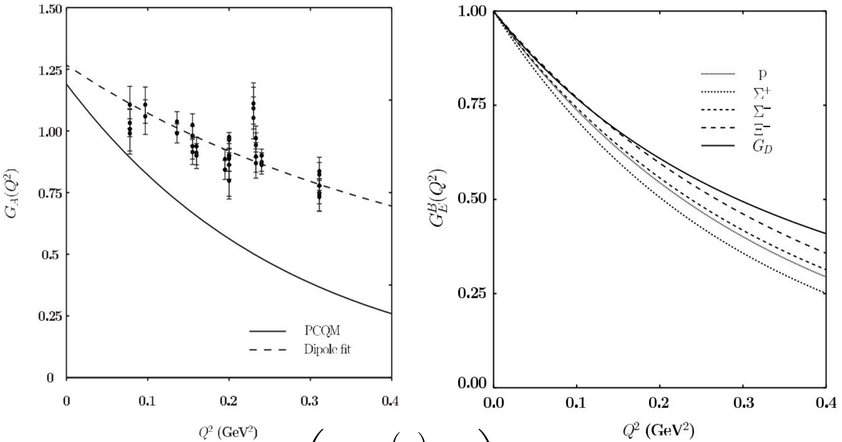

- $$u(\vec{x}) = \begin{pmatrix} g(r) \\ \mathrm{i}\vec{\sigma}\cdot\hat{x}f(r) \end{pmatrix} \chi_s \chi_f \chi_c.$$

$$g(r) = \exp\left(-\frac{\vec{x}^2}{2R^2}\right), f(r) = \frac{\rho r}{R}\exp\left(-\frac{\vec{x}^2}{2R^2}\right)$$

In our opinion

Due to Gaussian-type quark wavefunction, the theoretical predictions for the baryon form factors are consistent well with experimental data only at very low momentum transfer.

In our work

- The radial parts $g(r)$ and $f(r)$ are expanded in Sturmian basis

$$g(r) = \exp\Big(-\frac{\vec{x}^2}{2R^2}\Big) \rightarrow g(r) = \sum_n A_n \frac{S_{n0}(r)}{r},$$

$$f(r) = \frac{\rho r}{R}\exp\Big(-\frac{\vec{x}^2}{2R^2}\Big) \rightarrow f(r) = r\sum_n B_n \frac{S_{n0}(r)}{r},$$

where Sturmian functions

$$S_{nl} = \left[\frac{n!}{(n+2l+1)!}\right]^{1/2} (2br)^{l+1} e^{-br} L_n^{2l+1}(2br),$$

A_n, B_n, and b are free expansion parameters.

2. Electromagnetic form factor in the Perturbative Chiral Quark Model (PCQM)

Effective Lagrangian of the PCQM

$$\mathcal{L}_{\text{eff}}(x) = \mathcal{L}_{\text{inv}}(x) + \mathcal{L}_{\chi\text{SB}}(x)$$

- Chiral invariant Lagrangian

$$\mathcal{L}_{\text{inv}}(x) = \bar{\psi}(x)\Big\{ i\not{\partial} - \gamma^0 V(r) - \text{S}(r)\Big[\frac{U+U^\dagger}{2} + \gamma^5\frac{U-U^\dagger}{2}\Big]\Big\}\psi(x) + \frac{F^2}{4}\text{Tr}\left[\partial_\mu U \partial^\mu U^\dagger\right]$$

- Chiral symmetry breaking Lagrangian

$$\mathcal{L}_{\chi\text{SB}}(x) = -\bar{\psi}(x)\mathcal{M}\psi(x) - \frac{B}{2}\,\text{Tr}\left[\hat{\Phi}^2(x)\mathcal{M}\right]$$

- Model parameters

$$F = 88\text{ MeV}, \qquad B = 1.4\text{ GeV},$$
$$\mathcal{M} = \text{diag}\{m_u, m_d, m_s\} \to m_u = m_d = m_s/25 = \hat{m} = 7\text{ MeV}.$$

- Chiral invariant Lagrangian

$$\mathcal{L}_{\text{inv}}(x) = \underbrace{\bar{\psi}(x)[i\partial\!\!\!/ - \gamma^0 V(r)]\psi(x)}_{\mathcal{L}_q} + \underbrace{\frac{F^2}{4}\text{Tr}\left[\partial_\mu U \partial^\mu U^\dagger\right]}_{\mathcal{L}_\Phi}$$
$$\underbrace{-\bar{\psi}(x)\text{S}(r)\left[\frac{U+U^\dagger}{2} + \gamma^5 \frac{U-U^\dagger}{2}\right]\psi(x)}_{\mathcal{L}_{int}}$$

where $S(r)$: scalar potential, $V(r)$: vector potential

In SU(3) flavor symmetry

$$\text{q}-\text{field}: \ \psi(x) = \begin{pmatrix} u(x) \\ d(x) \\ s(x) \end{pmatrix}, \quad \chi-\text{field}: \ U = \exp\left[i\frac{\hat{\Phi}}{F}\right] \simeq 1 + i\frac{\hat{\Phi}}{F} + o\left(\frac{\hat{\Phi}}{F}\right),$$

$$\text{meson field}: \ \hat{\Phi} = \sum_{i=1}^{8} \Phi_i \lambda_i = \begin{pmatrix} \pi^0 + \frac{1}{\sqrt{3}}\eta & \sqrt{2}\pi^+ & \sqrt{2}K^+ \\ \sqrt{2}\pi^- & -\pi^0 + \frac{1}{\sqrt{3}}\eta & \sqrt{2}K^0 \\ \sqrt{2}K^- & \sqrt{2}\bar{K}^0 & -\frac{2}{\sqrt{3}}\eta \end{pmatrix}.$$

- Interaction Lagrangian

$$\begin{aligned}
\mathcal{L}_{\rm int}(x) &= -\bar{\psi}(x)\mathrm{S}(r)\left[\frac{U+U^{\dagger}}{2}+\gamma^5\frac{U-U^{\dagger}}{2}\right]\psi(x) \\
&= -\bar{\psi}(x)\mathrm{S}(r)\exp\left[i\gamma^5\frac{\hat{\Phi}}{F}\right]\psi(x) \\
&\color{red}{\downarrow}\quad \psi \to \exp\left[-i\gamma^5\frac{\hat{\Phi}}{2F}\right]\psi \\
&= -\bar{\psi}(x)\mathrm{S}(r)\psi(x) \\
&\quad \underbrace{+\frac{1}{2F}\partial_\mu\Phi_i(x)\bar{\psi}(x)\gamma^\mu\gamma^5\lambda^i\psi(x)+\frac{f_{ijk}}{4F^2}\Phi_i(x)\partial_\mu\Phi_j(x)\bar{\psi}(x)\gamma^\mu\lambda_k\psi(x)}_{\mathcal{L}_{\rm I}(x)},
\end{aligned}$$

Formulism

- Gell-Mann and Low theorem

$$\langle \hat{O} \rangle = {}^{B}\langle \phi_0 | \sum_{n=0}^{\infty} \frac{i^n}{n!} \int d^4x_1 \cdots d^4x_n T[\mathcal{L}_I(x_1) \cdots \mathcal{L}_I(x_n) \hat{O}] | \phi_0 \rangle_c^B,$$

. Interaction Lagrangian $\mathcal{L}_I(x)$

$$\mathcal{L}_I(x) = \frac{1}{2F} \partial_\mu \Phi_i(x) \bar{\psi}(x) \gamma^\mu \gamma^5 \lambda^i \psi(x) + \frac{f_{ijk}}{4F^2} \Phi_i(x) \partial_\mu \Phi_j(x) \bar{\psi}(x) \gamma^\mu \lambda_k \psi(x).$$

EM current operator

$$j^\mu = \bar{\psi}\gamma^\mu Q\psi + \left[f_{3ij} + \frac{f_{8ij}}{\sqrt{3}} \right] \Phi_i \partial^\mu \Phi_j + \left[f_{3ij} + \frac{f_{8ij}}{\sqrt{3}} \right] \frac{\Phi_j}{2F} \bar{\psi}\gamma^\mu \gamma^5 \lambda_i \psi + \bar{\psi}(Z-1)\gamma^\mu Q\psi$$

Feymann Diagrams

- Diagrams contributing to EM form factor

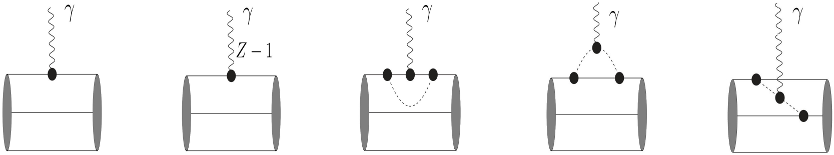

One loop diagram

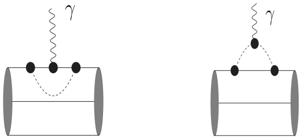

- Quark propagator

$$
\begin{aligned}
iG_\psi(x,y) &= \langle \phi_0 | T\psi(x)\bar{\psi}(y)|\phi_0\rangle \\
&= \sum_\alpha u_\alpha(\vec{x})u_\alpha(\vec{y})\exp[-i\mathcal{E}_\alpha(x_0-y_0)]\theta(x_0-y_0) \\
\text{in our calculation} &= u_0(\vec{x})u_0(\vec{y})\exp[-i\mathcal{E}(x_0-y_0)]\theta(x_0-y_0).
\end{aligned}
$$

- Meson propagator

$$
\begin{aligned}
i\Delta_{ij}(x-y) &= \langle 0|T\Phi_i(x)\Phi_j(y)|0\rangle \\
&= \delta_{ij}\int \frac{d^4k}{(2\pi)^4 i}\,\frac{exp[-ik(x-y)]}{M_\Phi^2-k^2-i\epsilon}.
\end{aligned}
$$

Theoretical results of charge FFs

$$
\begin{aligned}
G_E^B(Q^2)|_{LO} &= a_1^B G_E^p(Q^2)|_{LO}, \\
G_E^B(Q^2)|_{CT} &= \left[a_2^B(\hat{Z}-1) + a_3^B(\hat{Z}_s - 1)\right] G_E^p(Q^2)|_{LO}, \\
G_E^B(Q^2)|_{MC} &= \frac{1}{2(2\pi F)^2}\int_0^\infty dk \int_{-1}^{1} dx k^2(k^2 + kQx) F_{II}(k) F_{II}(k_+) t_E^B(k^2, Q^2, x)|_{MC}, \\
G_E^B(Q^2)|_{VC} &= \frac{1}{4(2\pi F)^2}\int_0^\infty dk k^4 F_{II}^2(k) G_E^p(Q^2)|_{LO}\left[\frac{a_6^B}{\omega_\pi^3(k^2)} + \frac{a_7^B}{\omega_K^3(k^2)} + \frac{a_8^B}{\omega_\eta^3(k^2)}\right], \\
G_E^B(Q^2)|_{MF} &\equiv 0,
\end{aligned}
$$

Theoretical results of magnetic FFs

$$
\begin{aligned}
G_M^B(Q^2)|_{LO} &= b_1^B \frac{m_B}{m_N} G_M^p(Q^2)|_{LO}, \\
G_M^B(Q^2)|_{CT} &= \left[b_2^B(\hat{Z}-1) + b_3^B(\hat{Z}_s - 1)\right] \frac{m_B}{m_N} G_M^p(Q^2)|_{LO}, \\
G_M^B(Q^2)|_{MC} &= \frac{5m_B}{6(2\pi F)^2}\int_0^\infty dk k^4 \int_{-1}^{1} dx (1-x^2) F_{II}(k) F_{II}(k_+) t_M^B(k^2, Q^2, x)|_{MC}, \\
G_M^B(Q^2)|_{VC} &= \frac{1}{2(2\pi F)^2}\int_0^\infty dk k^4 F_{II}^2(k) G_M^p(Q^2)|_{LO}\left[\frac{b_6^B}{\omega_\pi^3(k^2)} + \frac{b_7^B}{\omega_K^3(k^2)} + \frac{b_8^B}{\omega_\eta^3(k^2)}\right], \\
G_M^B(Q^2)|_{MF} &= \frac{m_B}{(2\pi F)^2}\int_0^\infty dk \int_{-1}^{1} dx k^4 (1-x^2) F_{II}(k) F_{II}(k_+) t_M^B(k^2, Q^2, x)|_{MF}.
\end{aligned}
$$

- Diagrams contributing to EM form factor

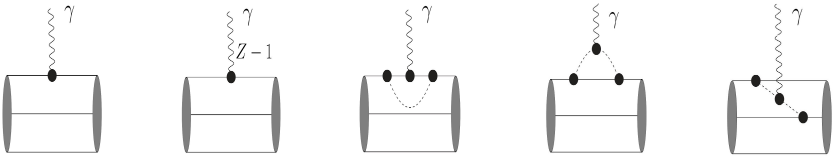

(a) (b) (c) (d) (e)

★ (a)-(d) contributing to charge FFs

★ (a)-(e) contributing to magnetic FFs

Considering

- the recent measurements of $G_E^p(Q^2)$ are in high precision
- only four diagrams contribute to $G_E^p(Q^2)$

We adjust our theoretical result of $G_E^p(Q^2)$ to experimental data.

3. Model quark wave function

In our work

- The radial parts $g(r)$ and $f(r)$ are expanded in Sturmian basis

$$g(r) = \exp\left(-\frac{\vec{x}^2}{2R^2}\right) \rightarrow g(r) = \sum_n A_n \frac{S_{n0}(r)}{r},$$

$$f(r) = \frac{\rho r}{R}\exp\left(-\frac{\vec{x}^2}{2R^2}\right) \rightarrow f(r) = r\sum_n B_n \frac{S_{n0}(r)}{r},$$

where Sturmian functions

$$S_{nl} = \left[\frac{n!}{(n+2l+1)!}\right]^{1/2} (2br)^{l+1} e^{-br} L_n^{2l+1}(2br),$$

Considering

- the recent measurements of $G_E^p(Q^2)$ are in high precision
- only four diagrams contribute to $G_E^p(Q^2)$

We adjust our theoretical result of $G_E^p(Q^2)$ to experimental data.

4. Results & Discussion

Quark wavefunction

- The expasion coefficients, A_n and B_n, are determined by adjusting the theoretical results of $G_E^p(Q^2)$ to the experimental data, in which the errors of the experimental data are considered.

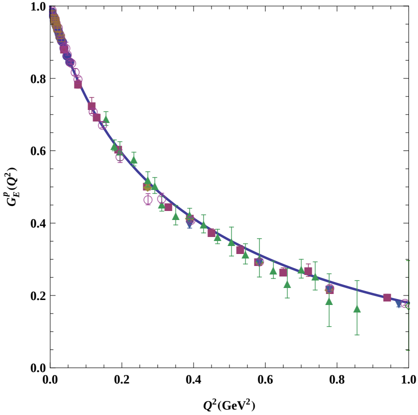

- The Sturmian function length parameter is fixed to be $b = 0.5\mathrm{GeV}$

n	A'_n	B'_n
0	0.21966 ± 0.00669	0.13892 ± 0.01405
1	-0.00817 ± 0.01204	0.02905 ± 0.00510
2	0.00073 ± 0.00107	0.01025 ± 0.00115
3	-0.01312 ± 0.00230	0.00072 ± 0.00086
4	-0.00853 ± 0.00150	-0.00092 ± 0.00016

Normalized radial wave functions

- Normalized radial wave functions of the valence quarks for the upper component $g(r)$ and the lower component $f(r)$.

n	A'_n	B'_n
0	0.21966 ± 0.00669	0.13892 ± 0.01405
1	-0.00817 ± 0.01204	0.02905 ± 0.00510
2	0.00073 ± 0.00107	0.01025 ± 0.00115
3	-0.01312 ± 0.00230	0.00072 ± 0.00086
4	-0.00853 ± 0.00150	-0.00092 ± 0.00016

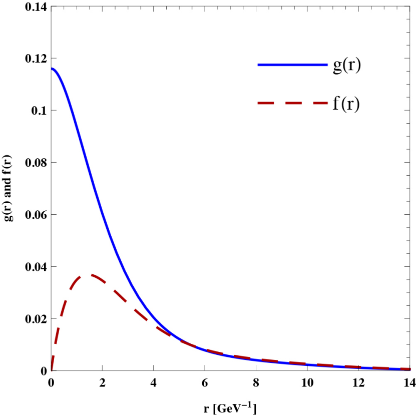

Charge form factors

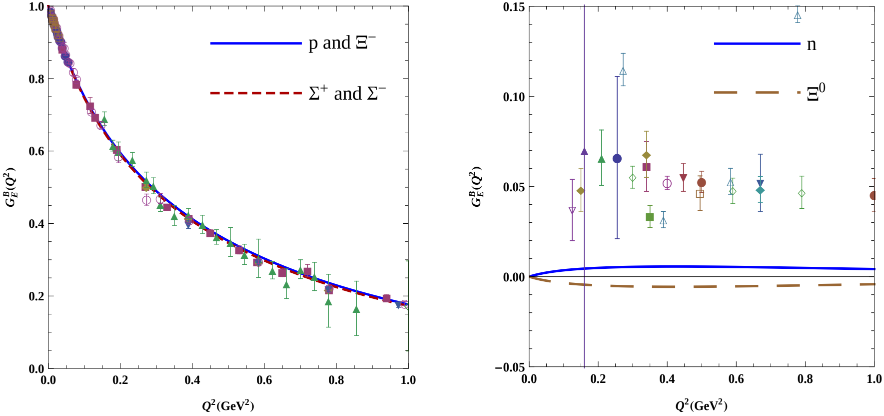

Neutral baryon charge form factors

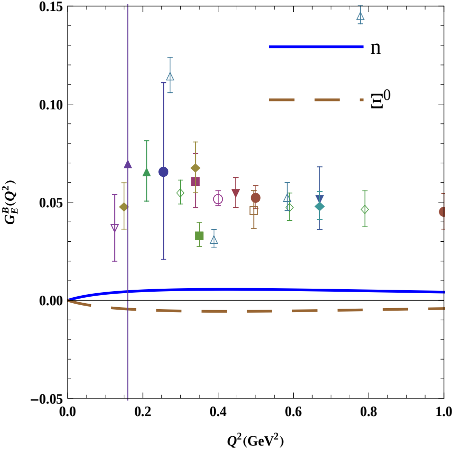

- $G_E^{n,\Xi^0}(Q^2)\big|_{LO} = 0$
- Meson cloud contributes
- Improvement
  - excited quark propagator

Octet baryon mean-square charge radii

$$\langle r_E^2 \rangle^{B^\pm} = -\frac{6}{G_E^{B^\pm}(0)} \frac{d}{dQ^2} G_E^{B^\pm}(Q^2)\Big|_{Q^2=0}, \quad \langle r_E^2 \rangle^{B^0} = -6 \frac{d}{dQ^2} G_E^{B^0}(Q^2)\Big|_{Q^2=0}$$

	3q LO+CT	Meson loops MC+VC	Total	Exp.
$\langle r_E^2 \rangle^p$	0.710	0.057	0.767 ± 0.113	0.76 ± 0.09
$\langle r_E^2 \rangle^n$	0	-0.014	-0.014 ± 0.001	-0.116 ± 0.002
$\langle r_E^2 \rangle^{\Sigma^+}$	0.701	0.080	0.781 ± 0.108	–
$\langle r_E^2 \rangle^{\Sigma^0}$	-0.009	0.009	0	–
$\langle r_E^2 \rangle^{\Sigma^-}$	0.718	0.063	0.781 ± 0.108	0.61 ± 0.21
$\langle r_E^2 \rangle^{\Lambda}$	-0.009	0.009	0	–
$\langle r_E^2 \rangle^{\Xi^0}$	-0.017	0.031	0.014 ± 0.008	–
$\langle r_E^2 \rangle^{\Xi^-}$	0.727	0.040	0.767 ± 0.113	–

§ J. Beringer et al. (Particle Data Group) Phys. Rev. D86, 010001 (2012).

Magnetic form factors

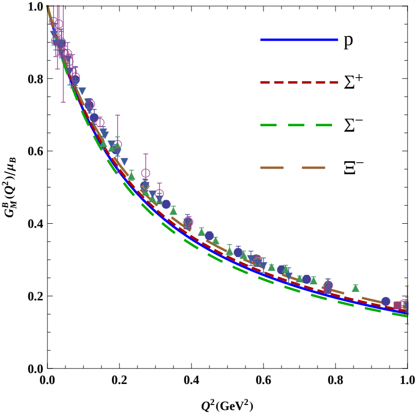

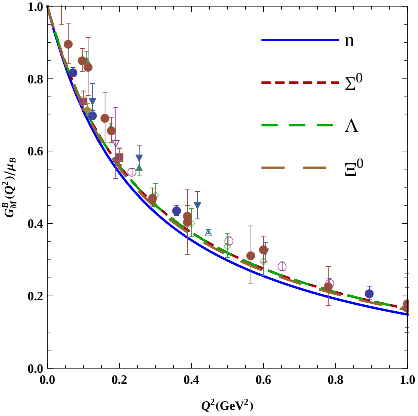

Octet baryon magnetic moments

$\mu_B = G_M^B(0)$

	3q LO+CT	Meson loops MC+VC+MF	Total	Exp.
μ_p	2.290	0.445	2.735 ± 0.121	2.793
μ_n	-1.527	-0.429	-1.956 ± 0.103	-1.913
μ_{Σ^+}	2.299	0.238	2.537 ± 0.201	2.458 ± 0.010
μ_{Σ^0}	0.773	0.065	0.838 ± 0.091	–
μ_{Σ^-}	-0.754	-0.107	-0.861 ± 0.040	-1.160 ± 0.025
μ_{Λ}	-0.791	-0.076	-0.867 ± 0.074	-0.613 ± 0.004
μ_{Ξ^0}	-1.564	-0.126	-1.690 ± 0.142	-1.250 ± 0.014
μ_{Ξ^-}	-0.800	-0.040	-0.840 ± 0.087	-0.651 ± 0.080
$\mu_{\Sigma^0\Lambda}$	-1.322	-0.277	-1.599 ± 0.068	-1.610 ± 0.080

§ J. Beringer et al. (Particle Data Group) Phys. Rev. D86, 010001 (2012).

Octet baryon mean-square magnetic radii

$$\langle r_M^2 \rangle^B = -\frac{6}{G_M^B(0)} \frac{d}{dQ^2} G_M^B(Q^2) \Big|_{Q^2=0}$$

	3q LO+CT	Meson loops MC+VC+MF	Total	Exp.
$\langle r_M^2 \rangle^p$	0.748	0.161	0.909 ± 0.084	0.74 ± 0.10
$\langle r_M^2 \rangle^n$	0.698	0.224	0.922 ± 0.079	0.76 ± 0.02
$\langle r_M^2 \rangle^{\Sigma^+}$	0.810	0.075	0.885 ± 0.094	–
$\langle r_M^2 \rangle^{\Sigma^0}$	0.824	0.027	0.851 ± 0.102	–
$\langle r_M^2 \rangle^{\Sigma^-}$	0.783	0.168	0.951 ± 0.083	–
$\langle r_M^2 \rangle^{\Lambda}$	0.815	0.037	0.852 ± 0.103	–
$\langle r_M^2 \rangle^{\Xi^0}$	0.827	0.044	0.871 ± 0.099	–
$\langle r_M^2 \rangle^{\Xi^-}$	0.851	−0.011	0.840 ± 0.109	–
$\langle r_M^2 \rangle^{\Sigma^0\Lambda}$	0.739	0.174	0.913 ± 0.083	–

§ J. Beringer et al. (Particle Data Group) Phys. Rev. D86, 010001 (2012).

Summary

- Quark WF has been determined by fitting theoretical results of proton charge form factor numerically to experimental data.

- EM form factors of octet baryons have been studied in the PCQM with the predetermined quark WF.

- Results are in good agreement with experimental data, except $G_E^n(Q^2)$.

- Therefore, the predetermined quark WF reflects physics suitable and reasonable for the PCQM.

Outlook

- Axial form factor of baryons in the PCQM with the predetermined quark WF
- The properties of decuplet baryons in the PCQM with the predetermined quark WF
- The neutral baryon charge form factors with excited-state quarks

♠ We expect that results are also in good agreement with experimental data.

Thank you !!!